NEACRP-L-182
(USA)
June 1977

POTENTIAL AND LIMITATION OF THE HETEROGENEOUS REACTOR CONCEPT

by

W. P. Barthold, J. Beitel, E. Khan, and C. Tzanos

LMFBRs with internal blankets, often called "heterogeneous" or "parfait" reactors received substantial attention during the last two years. The general conclusion was that heterogeneous reactor configurations will not only increase the breeding ratio but also lower the doubling time and improve the safety characteristics of the reactor. A more detailed investigation of heterogeneous cores shows that there is not just a heterogeneous reactor concept but that there is a great variety of heterogeneous cores depending on the arrangement of the internal blankets in the core region. The blanket region usually separates the core regions from each other. A basic characteristic of heterogeneous cores is then the degree of neutronic coupling between different core zones. Some of the heterogeneous core configurations[1-2-3] used blanket assemblies as fixed shim assemblies to shape the power. In this case, the coupling between different core regions is very tight. The breeding performance, for example, of such a system is equivalent to that of a homogeneous system which has the same homogenized volume fractions[3]. Improvements often seen in the breeding performance of LMFBRs by introducing internal blankets[1-2-3] can be attributed to the increase in homogenized fuel volume fractions[3] which comes close to an optimum fuel volume fraction[4]. As more heavy metal is packed into the core in the form of internal blanket assemblies, the breeding ratio will

steadily increase as the homogenized fuel volume fraction increases. For as long as the increase in breeding gain is greater than the increase in fissile inventory the doubling time will be decreasing. However, this reduction in doubling time can also be achieved by using larger pin diameters in the homogeneous design. Introducing internal blankets into such an optimized regular core will lead to an increase in doubling time[3].

The transition from a tightly coupled to a very loosely coupled core comes when the thickness of the internal blankets increases which separate the core regions. While one row of blanket assemblies will still permit tight coupling, the addition of a second row of internal blankets will lead to a system of nearly uncoupled small reactors[5]. The increase in the leakage component and the reduction in the spectral component lead to an overall reduction of the sodium void reactivity. It is this feature which makes heterogeneous reactors particularly attractive from the safety point of view[6-9]. In an unprotected loss-of-flow transient in a large LMFBR the voiding of the coolant may result in very large reactivity ramp rates leading to energy release rates which could exceed the design limits of the containment[6]. The incentive for the design is then to develop core configurations which have very low sodium void reactivities. The following discussion will be limited to a performance evaluation of low sodium void cores vs. homogeneous cores.

It was found that a low sodium void core consisting of fuel assemblies with a flat-to-flat distance between 6-7 inches can be constructed in the following way[5]: a center core configuration has a 4-row inner core, followed by 2 rows of internal blanket assemblies which are followed by

3 rows of fuel, 2 rows of blanket, etc. A center blanket core layout can be designed in the following way: a 3-row center blanket is surrounded by 3 rows of fuel assemblies, 2 rows of blanket assemblies, 3 rows of fuel assemblies, etc. The characteristic of a homogeneous 1200 MWe oxide LMFBR was compared with that of low sodium void ~~homo~~heterogeneous cores of the same power output. Heterogeneous cores have some features which distinguish them from homogeneous cores.

(a) Lower sodium void reactivity ($2 vs. $7)

(b) Higher breeding ratio (1.35 - 1.40 compared to less than 1.30)

(c) Higher doubling times (18 years vs. 14 years)

(d) Higher fissile inventories (30% higher and more)

(e) Larger core sizes (more than 100 additional assemblies)

(f) Lower Doppler coefficients (for example, -0.005 vs. -0.009)

(g) Higher enrichments

(h) Lower damage fluxes (more than 20% reduction)

(i) Reduced control rod worth

(j) For the same number of orificing zones, higher clad midwall temperatures (20°F and more)[11]

(k) Higher fuel compaction reactivity (for example 0.0058 Δk/k vs. 0.0042 Δk/k)

(l) Localized reactivity addition gives rise to localized power peaks

(m) Less sensitivity of doubling times and sodium void reactivity to changes in fuel pin diameters[12]

(n) Greater sensitivity of power peaking and sodium void reactivity to small changes in enrichment split[10]

(o) Lower total inelastic strain in cladding (2% vs. 3%)

The analysis of heterogeneous cores is more difficult than the analysis of homogeneous cores because of

(a) Neutronic decoupling of core zones

(b) Need for transport calculations instead of diffusion calculations to obtain accurate flux and power distributions

(c) Significance of γ heating in internal blankets

For the analysis and design of heterogeneous cores we need modified design approaches, and analysis tools. However, no problems could be identified so far which would affect the feasibility of heterogeneous cores.

REFERENCES

1. J. C. Mouguiot et al., "Breeding Gains of Sodium-Cooled Oxide Fast Reactors," Trans. Am. Nucl. Soc. 20, 348 (1975), also ORNL-TR-2294

2. U. Wehmann, H. Spenke, "Vorstellung eines 1200 MWe Natrium Brueters mit internen Brutzonen," Reaktortagung Duesseldorf (1976).

3. Y. Chang, W. P. Barthold, and C. E. Till, "An Evaluation of the Cylindrical Parfait Core Concept," FRA-TM-88 (April 19, 1976).

4. R. B. Turski, W. P. Barthold, "Optimum Pin Diameters for 1200 MWe Oxide LMFBRs Using CW316SS as Structural Material," Trans. Am. Nucl. Soc. 23, 435-436 (1976).

5. C. P. Tzanos, W. P. Barthold, "A Systematic Approach for Constructing Low Sodium Void Heterogeneous Core," ANS Meeting, June 12-17, 1977.

6. C. P. Tzanos, W. P. Barthold, et al., "Design-Related Inherent Safety Characteristics in Large LMFBR Power Plants," Proc. International Meeting on Fast Reactor Safety and Related Physics," Chicago CONF-761001 (1976).

7. J. B. van Erp, W. P. Barthold, C. P. Tzanos, "Inherent Safety of Large LMFBR Power Plants," Trans. Am. Nucl. Soc. 23, 376-377 (1976).

8. M. J. Driscoll, et al., "Safety and Breeding-Related Aspects of Fast Reactor Cores Having Internal Blankets," Proc. International Meeting on Fast Reactor Safety and Related Physics, Chicago, CONF-761001 (1976).

9. U. Wehmann, "Safety Aspects in Nuclear Core Design of LMFBRs," Proc. International Meeting on Fast Reactor Safety and Related Physics, Chicago CONF-761001 (1976).

10. C. P. Tzanos, W. P. Barthold, "Sensitivity of Power Distribution in Large Heterogeneous LMFBR Designs," ANS Meeting, June 12-17, 1977.

11. E. Khan, W. P. Barthold, "Flow Orificing of Large LMFBRs with Interassembly Heat Transfer," ANS Meeting, June 12-17, 1977.

12. Y. Orechwa, R. Turski, M. King, "Pin Diameter Optimization in Heterogeneous vs. Homogeneous Cores," ANS Meeting, June 12-17, 1977.

APPENDIX A

The accompanying article was prepared for presentation at the June 1977 meeting of the American Nuclear Society. Because of word limitations most of the technical data upon which the conclusions in the article are based were not included. Some of this supporting information has been assembled from a number of different ANL internal reports and is presented in this Appendix.

Most of the information in the following tables and figures is based on calculations of 1200 MWe oxide LMFBR designs. The designs are defined in Tables I, II and III. The important characteristics of these heterogeneous cores were summarized in the article. In the section below several of the characteristics listed in the article have been repeated. These are then followed by a listing of the tables which contain information which tend to support the particular conclusion.

a. Lower Sodium Void Reactivity ($2 vs $7). See Tables IV, V, VI and VII.

c. High Doubling Times (18 years vs 14 years). See Tables VIII and IX.

d. High Fissile Inventories (30% higher and more). See Table VIII.

f. Lower Doppler Coefficient (For Example, -0.005 vs -0.009). See Table X.

i. Reduced Control Rod Worth. See Table XI.

In addition to the above tables several figures presenting results from the heterogeneous core analysis are also included. They are:

Fig. 1. Sodium Void Reactivity as a Function of Internal Blanket Thickness (Equal Power Peaks for Inner and Outer Core Zones) Geometry 1C.

Fig. 2. Power Distribution for Geoemtry 1B.

Fig. 3. Sodium Void Reactivity as a Function of Blanket Position.

Fig. 4. Distribution of Sodium Void for Reference Geometry.

Fig. 5. Distribution of Sodium Void for Geometry 1B.

Fig. 6. Distribution of Sodium Void for Geometry 2 (Two Internal Blanket Rings).

Fig. 7. Core Layout for 1200 MWe Oxide LMFBR.

In Fig. 1. the decrease in sodium void reactivity with increasing blanket thickness is shown. As the blanket thickness is increased the negative leakage component of the sodium void becomes relatively more important. The power distribution in one of the cores with a single thick internal blanket ring, case 1B, is shown in Fig. 2. In Fig. 3 it is shown that the sodium-void reactivity decreases somewhat as the radius of the internal blanket ring is increased. Figs. 4, 5 and 6 show the radial distribution of sodium reactivity in the reference core, in a heterogeneous core with one internal blanket ring (Case 1B), and in a heterogeneous core with two internal blanket rings (Geometry 2). The reduction in sodium void in the heterogeneous designs is indicated by comparison of these figures. Fig. 7 gives the cross section layout for the reference 1200 MWe oxide design.

TABLE I. 1200 MWe Oxide LMFBR Design Characteristics
0.30 in. Fuel Pin Diameter

Core Parameters

Power, MWT	3019.
Maximum Sodium velocity, ft/sec	28.0
Temperature rise across core, deg. F	280.0
Sodium Outlet temperature, deg. F	1000.0
Active core height, in.	40.0
Sodium gap between assemblies, in.	0.310
Pressure drop across assembly, psi (fuel bundle only)	67.
Assembly pitch, in.	6.548
Number of fuel assemblies	402
Number of control rod positions	19
Number of rows in core	12
Driver/blanket residence time, cycles	2/5
Cycle length, fpd	300

Subassembly Design

	Driver	Blanket
Active height, in.	40.0	70.0
Axial blanket thickness, in.	15.0	-
Axial reflector thickness, in.	3.0	3.0
Plenum length, in.	40.0	40.0
Structural material	CW316SS	CW316SS
Maximum linear heat rating, kW/ft	13.5	13
Fuel pin diameter, in.	0.300	0.600
Fuel cladding thickness, in.	0.018	0.020
Fuel pin pitch/diameter, in.	1.208	1.053
Spacer wire thickness, in.	0.063	0.032
Number of Fuel Pins per Assembly	271	91
Duct Thickness, In.	0.135	0.135
Fuel Smear Density, %T.D.	88.0	95.0
Volume Fractions		
Fuel	0.3845	0.5975
Total Coolant	0.3848	0.2412
Structure	0.2157	0.1613

TABLE II. 1200 MWe Oxide LMFBR Design Characteristics
0.33 in. Fuel Pin Diameter

Core Parameters

Power, MWT	3019.
Maximum sodium velocity, ft/sec	28.
Temperature rise across core, deg. F	280.
Sodium outlet temperature, deg. F	1000.
Active core height, in.	40.
Sodium gap between assemblies, in.	0.230
Pressure drop across assembly, psi (fuel bundle only)	82.
Assembly pitch, in.	6.832
Number of fuel assemblies	402
Number of control rod positions	19
Number of rows in core	12
Driver/blanket residence time, cycles	2/5
Cycle length, fpd	300

Subassembly Design

	Driver	Blanket
Active height, in.	40.0	70.0
Axial blanket thickness, in.	15.0	-
Axial reflector thickness, in.	3.0	3.0
Plenum length, in.	40.0	40.0
Structural material	CW316SS	CW316SS
Maximum linear heat rating, kW/ft	13.5	13.
Fuel pin diameter, in.	0.330	0.600
Fuel cladding thickness, in.	0.020	0.020
Fuel pin pitch/diameter, in.	1.141	1.058
Spacer wire thickness, in.	0.046	0.035
Number of fuel pins per assembly	271.	91.
Duct thickness, in.	0.157	0.218
Fuel smear density, %T.D.	88.	95.
Volume Fractions		
Fuel	0.4440	0.5975
Total coolant	0.3286	0.2412
Structure	0.2274	0.1613

Table III. Description of the One-Dimensional Configuration of the 1200 MWe LMFBR

Configuration	Number of Rings of Internal Blankets	Location of Internal Blankets, Rows
1A	1	4-5
1B	1	6-7
1C	1	8-9
1D	1	10-11
1E	1	11-12
2	2	1-3,7-8
3	2	1-3,8-9
4	2	5-6,10-11

TABLE IV. Enrichments, Radial Power Peaking Factors, Reactivity Changes Due to Voiding the Core of 1 cm Height at the Midplane

Case	E_1	E_2/E_1	E_{AVG}	Radial Power Peaking Factor	$\Delta k \times 10^{-6}$	$\Delta k/\Delta k_{ref}$
Reference Core	13.008	1.300	14.6	1.203	371.09	1.00
One Blanket Zone						
1A Blanket in Rows 4&5	21.251	0.700	15.2	1.329	294.58	0.79
1B Blanket in Rows 6&7	16.169	0.980	16.0	1.300	244.35	0.66
1C Blanket in Rows 8&9	14.639	1.220	16.8	1.311	208.04	0.56
1D Blanket in Rows 10&11	13.956	1.654	18.1	1.371	196.93	0.53
1E Blanket in Rows 11&12	13.756	2.20	19.0	1.432	196.36	0.53

TABLE V. Components of Sodium Void Reactivity

	Sodium Void Reactivity ($\Delta k/k/kg \times 10^6$ at Midplane					
	Inner Core			Outer Core		
Case	Leakage	Spectral	Total	Leakage	Spectral	Total
1A	-4.51	6.53	2.02	-2.84	12.80	9.96
1B	-3.53	9.98	6.45	-3.63	11.84	8.21
1C	-2.39	11.65	9.26	-4.63	10.42	5.79
1D	-1.60	12.09	10.49	-5.25	7.71	2.46
1E	-0.96	12.92	11.96	-6.65	7.54	0.89
Reference	-0.0003	16.94	16.94	-9.01	13.48	4.47

TABLE VI. Enrichments, Radial Power Peaking Factors, Reactivity Changes Due to Voiding the Core of 1 cm Height at the Midplane

Case	E_1	E_2/E_1	E_{AVG}	Radial Power Peaking Factor	$\Delta k \times 10^{-6}$	$\Delta k/\Delta k_{ref}$
Two Blanket Zones						
2 Blanket in Rows 1-3, 7&8	17.758	0.980	17.5	1.197	190.64	0.51
3 Blanket in Rows 1-3, 8&9	16.517	1.150	18.1	1.187	178.20	0.48
4 Blanket in Rows 5&6, 10&11	17.564	1.150, 1.140	19.8	1.154	134.27	0.36

TABLE VII. Enrichments, Radial Power Peaking Factors, Reactivity Changes Due to Voiding the Core of 1 cm Height at the Midplane

Configuration	Internal Blanket Location, rows	ϵ_1	ϵ_2/ϵ_1	$\bar{\epsilon}$	Power Peaking Factor	Sodium Void Reactivity
Reference	-	13.0	1.300	14.6	1.203	1.00
1B	6-7	16.17	0.98	16.0	1.300	0.66
2	1-3, 7-8	17.76	0.98	17.5	1.197	0.51

TABLE VIII. Breeding Performance of the Reference Reactor and Heterogeneous Reactor With Center Blanket and Center Core

	0.30" Pin Reference			0.30" Pin Heterogeneous Central Blanket			0.30" Pin Heterogeneous Central Core Split 1.156/1.162			0.30" Pin Heterogeneous Central Core Split 1.14/1.17			0.30" Pin 5 Zone Core-Equivalent to Heterogeneous Central Core		
	BOEC	EOEC	EOEC-BOEC	EOEC	EOEC	EOEC-BOEC	BOEC	EOEC	EOEC-BOEC	BOEC	EOEC	EOEC-BOEC	BOEC	EOEC	EOEC-B
Fissile Inventory, kg															
Core															
^{239}Pu	3595.4	3564.1	-31.3	4256.2	4093.5	-192.7	4603.4	4350.4	-253.0	4633.7	4364.8	-268.9	4865.8	4587.2	-278.6
^{241}Pu	486.8	393.4	-93.4	607.2	509.6	-98.0	659.2	558.0	-101.2	663.5	559.9	-103.6	698.6	596.7	-101.9
Axial Blanket															
^{239}Pu	126.5	371.5	245.0	78.2	230.8	152.6	67.8	199.8	132.0	68.2	201.3	133.1	62.8	185.3	122.5
^{241}Pu	-	0.1	0.1	-	-	-	-	-	-	-	-	-	-	-	-
Radial Blanket															
^{239}Pu	397.6	587.5	189.9	555.2	1011.1	455.9	599.1	1161.8	562.7	601.7	1182.4	580.7	600.8	1213.0	612.2
^{241}Pu	0.1	0.1	0.0	0.2	0.7	0.5	0.3	0.9	0.6	0.3	1.01	0.7	0.2	1.0	0.8
Total	4606.4	4916.7	310.3	5527.4	5845.7	318.3	5929.8	6270.9	341.1	5967.4	6309.4	342.4	6228.2	6583.5	355.3
k_{eff}	1.024	1.000	-0.024	1.028	1.000	-0.028	1.024	1.000	-0.024	1.024	1.000	-0.024	1.025	1.000	-0.0
RDT, yrs.	14.81			17.4			17.4			17.4			17.5		
CSDT, yrs.	16.86			20.7			20.7			20.7			20.7		
Reactivity Change for Voiding Core, % Δk	2.041	2.099		0.346	0.399		0.427	0.834		0.443	0.679		0.701	1.083	
Reactivity Change for Voiding Internal Blanket, % Δk				0.098	0.150		0.141	0.222		0.137	0.218		0.583	0.652	

TABLE IX. Breeding Performance of a 1200 MWe Oxide Regular and Parfait Design Based on a 0.330 in. o.d. Fuel Pin (control rods are excluded)

	Regular Configuration			Heterogeneous Central Core		
	BOEC	EOEC	EOEC-BOEC	BOEC	EOEC	EOEC-BOEC
Fissile Inventory, kg						
Core						
^{239}Pu	4038.8	4073.6	34.8	5109.2	4932.0	-177.2
^{241}Pu	547.0	449.7	-97.3	727.8	622.9	-104.9
Axial Blanket						
^{239}Pu	118.1	348.6	230.5	69.6	206.1	136.5
^{241}Pu	-	0.1	0.1	-	-	-
Radial Blanket						
^{239}Pu	354.6	524.0	169.4	562.6	1085.1	522.5
^{241}Pu	-	0.1	0.1	0.2	0.6	0.4
Total	5058.5	5396.1	337.6	6469.4	6846.7	377.3
k_{eff}	1.013	1.000	-0.013	1.020	1.000	-0.020
RDT, yrs.	14.98			17.15		
CSDT, yrs.	17.32			20.37		

TABLE X. Average Core Fissile Enrichments, Doppler Coefficients and Compaction Reactivities

	Homogeneous	Heterogeneous Core	Heterogeneous Internal Blankets
Enrichment, %	12.7	17.2	24.3
Doppler Coeff., $T\frac{dk}{dT} \times 10^{-4}$	97.9	56.8	
Compaction Δk	0.0042	0.0058	

TABLE XI. Central Control Rod Reactivity Worth for Different Internal Blanket Thicknesses

Internal Blanket Thickness No. of Rows	Control Rod Worth Δk
1	0.00282
2	0.00130
3	0.00044

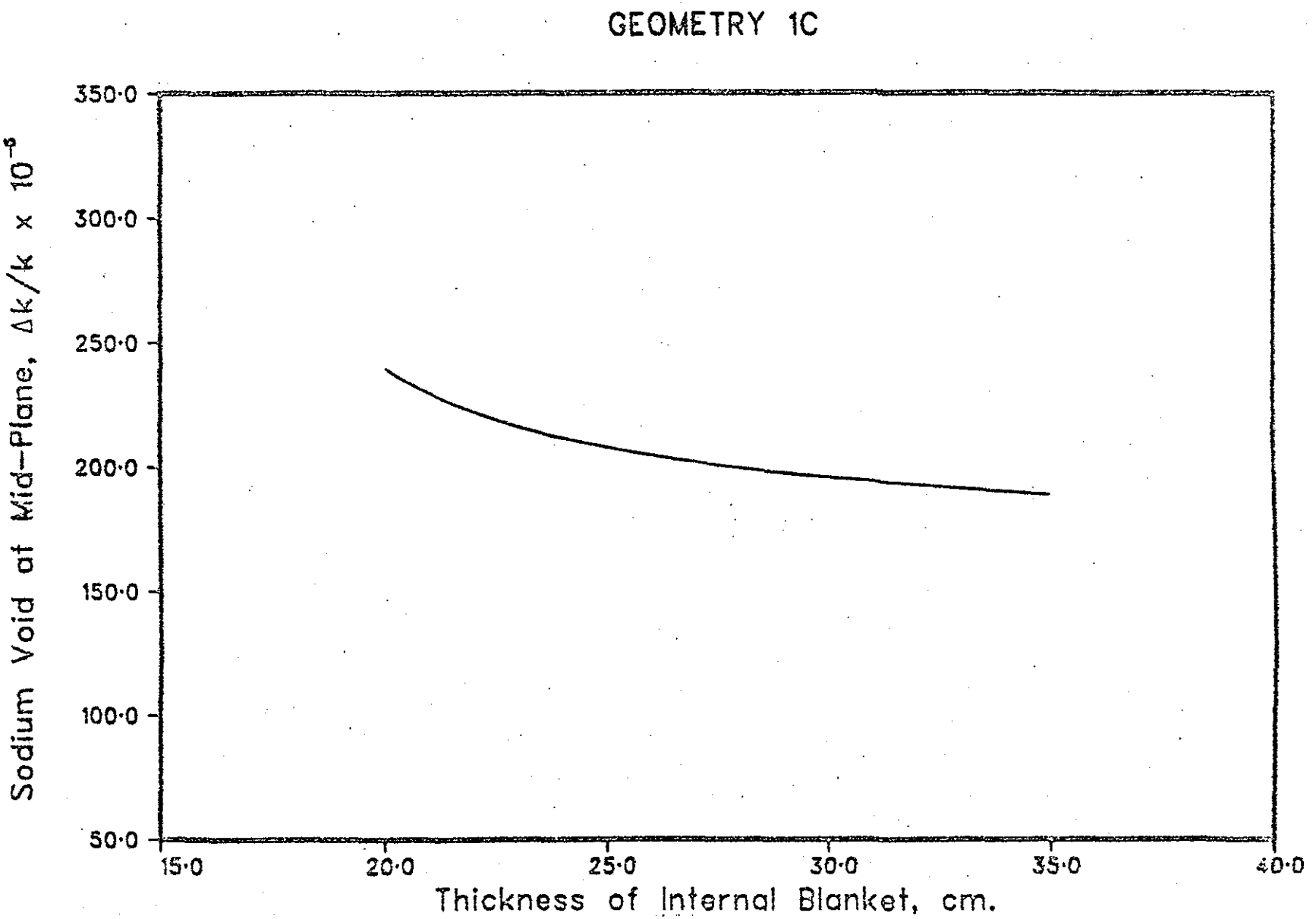

Fig. 1. Sodium Void Reactivity as a Function of Internal Blanket Thickness (Equal Power Peaks for Inner and Outer Core Zones) Geometry 1C

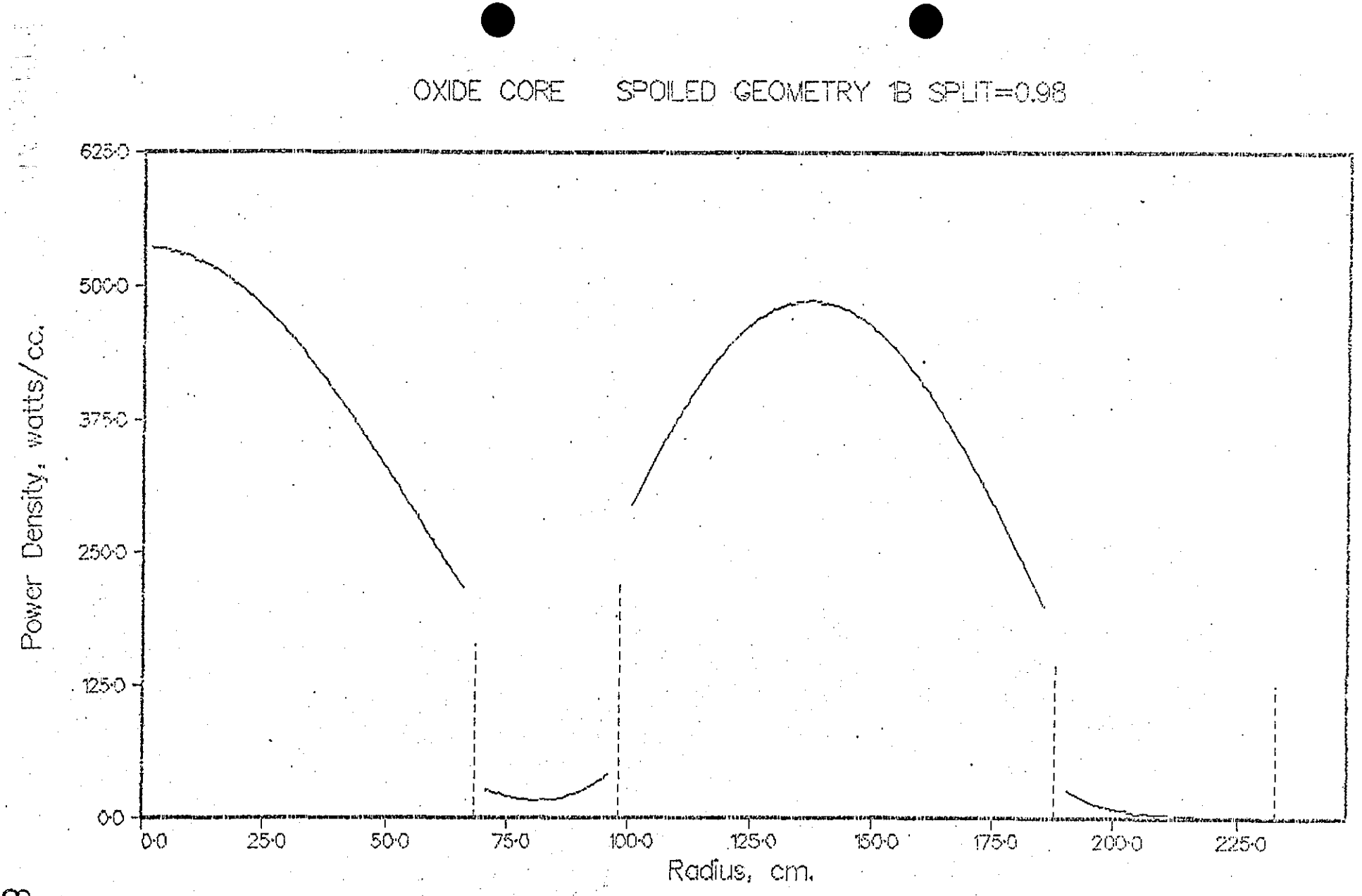

Fig. 2. Power Distribution for Geometry 1B

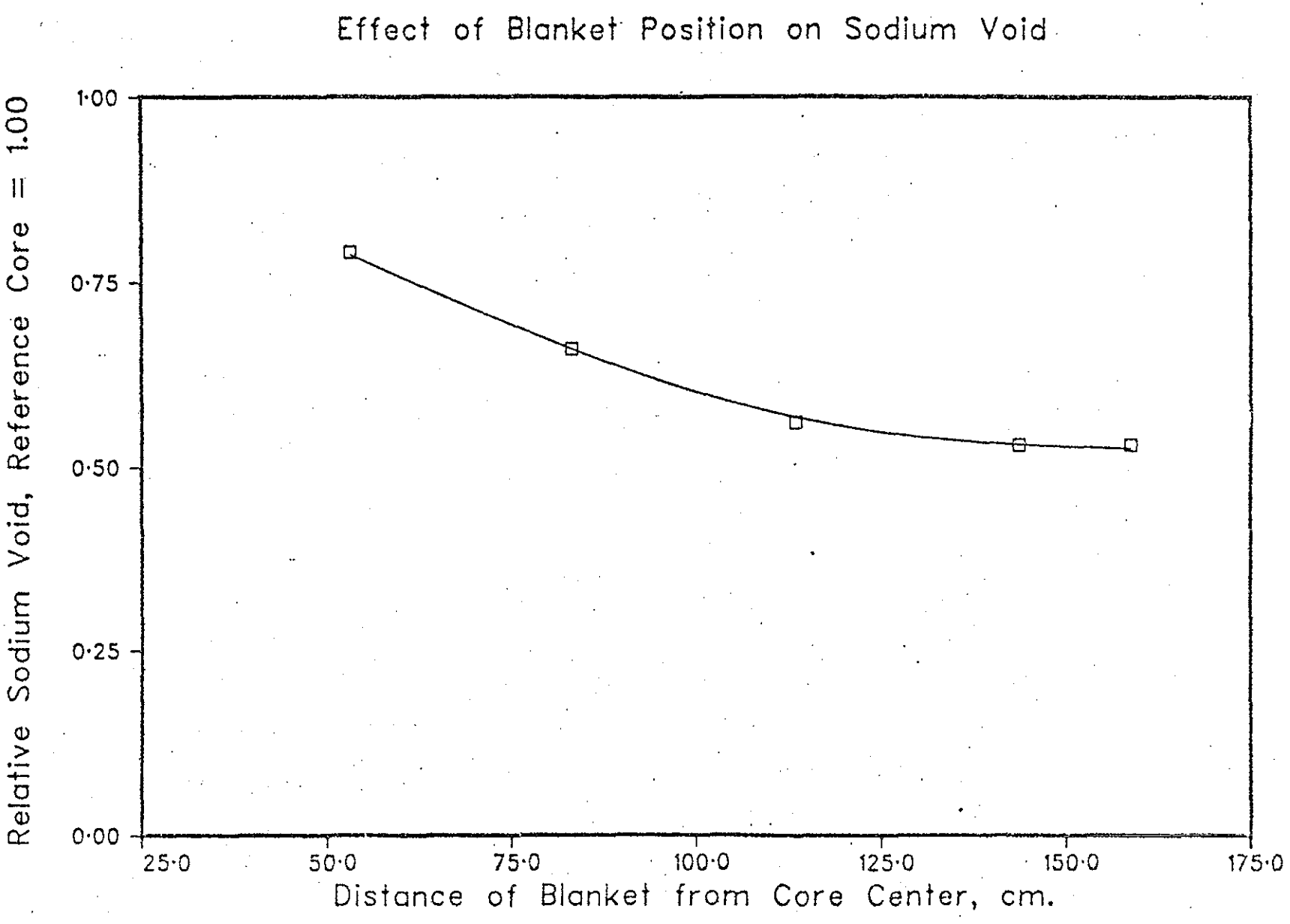

Fig. 3. Sodium Void Reactivity as a Function of Blanket Position

Fig. 4. Distribution of Sodium Void Reactivity for Reference Geometry

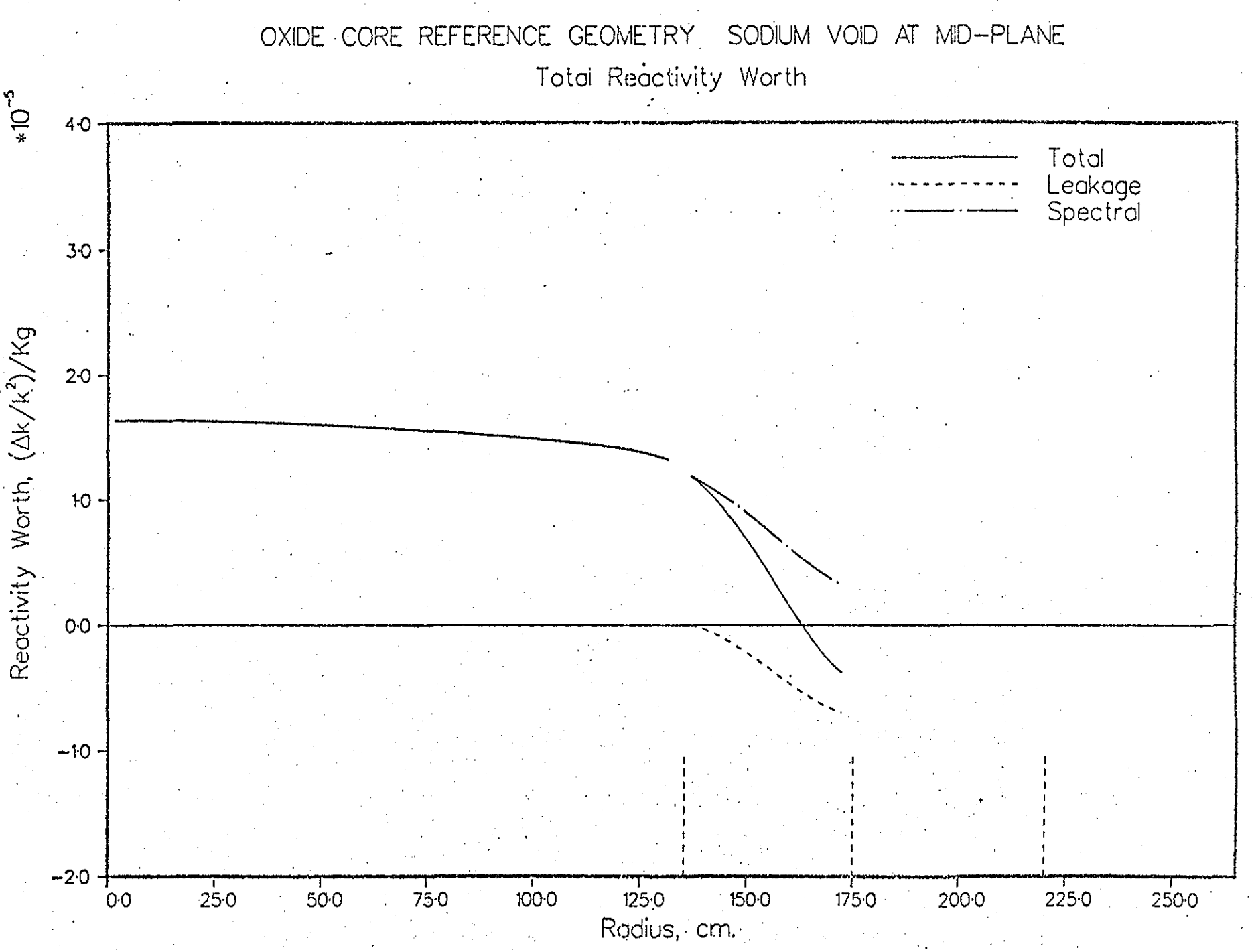

Fig. 5. Distribution of Sodium Void Reactivity for Geometry 1B

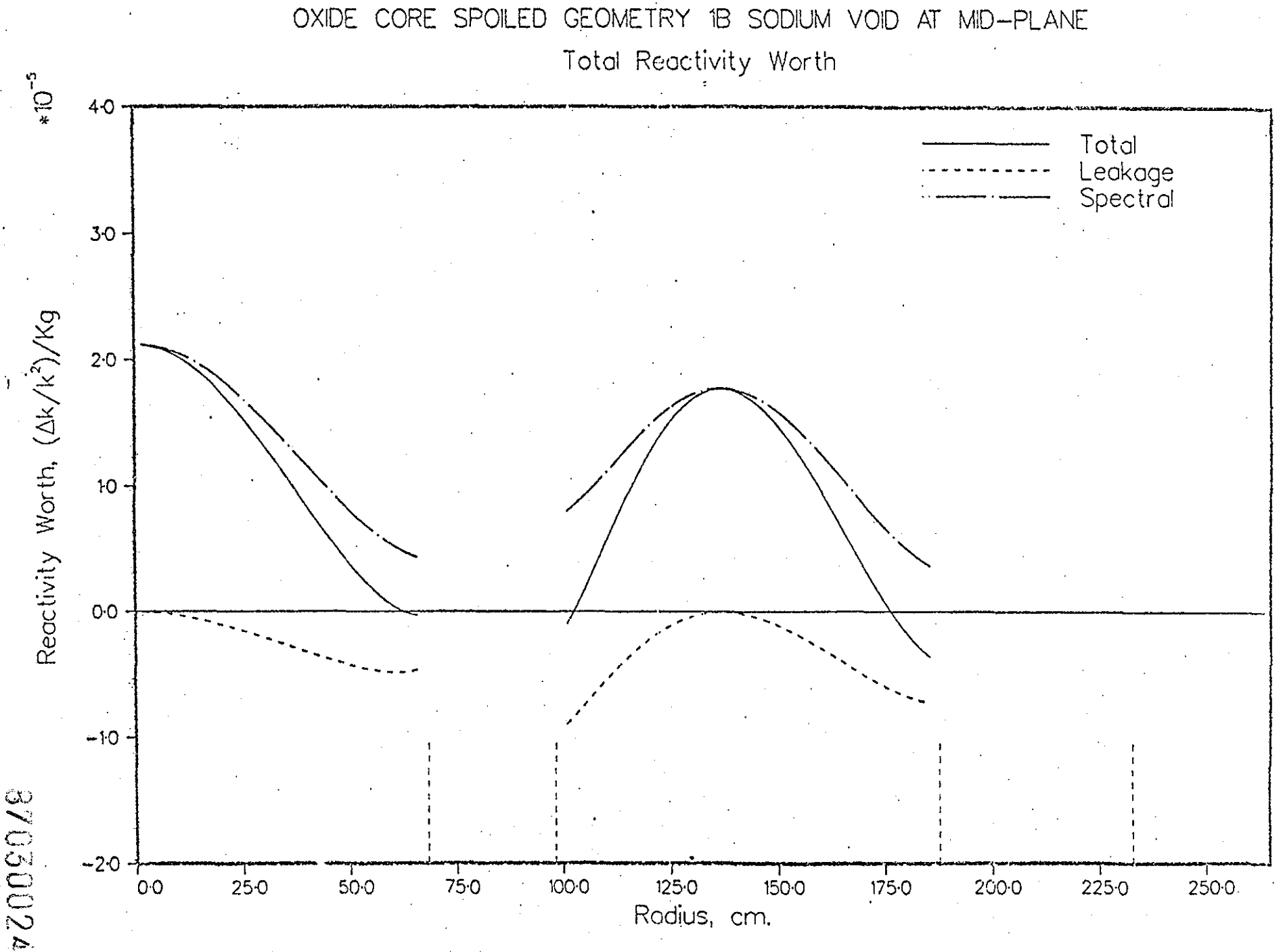

Fig. 6. Sodium Void Reactivity Distribution for Geometry 2

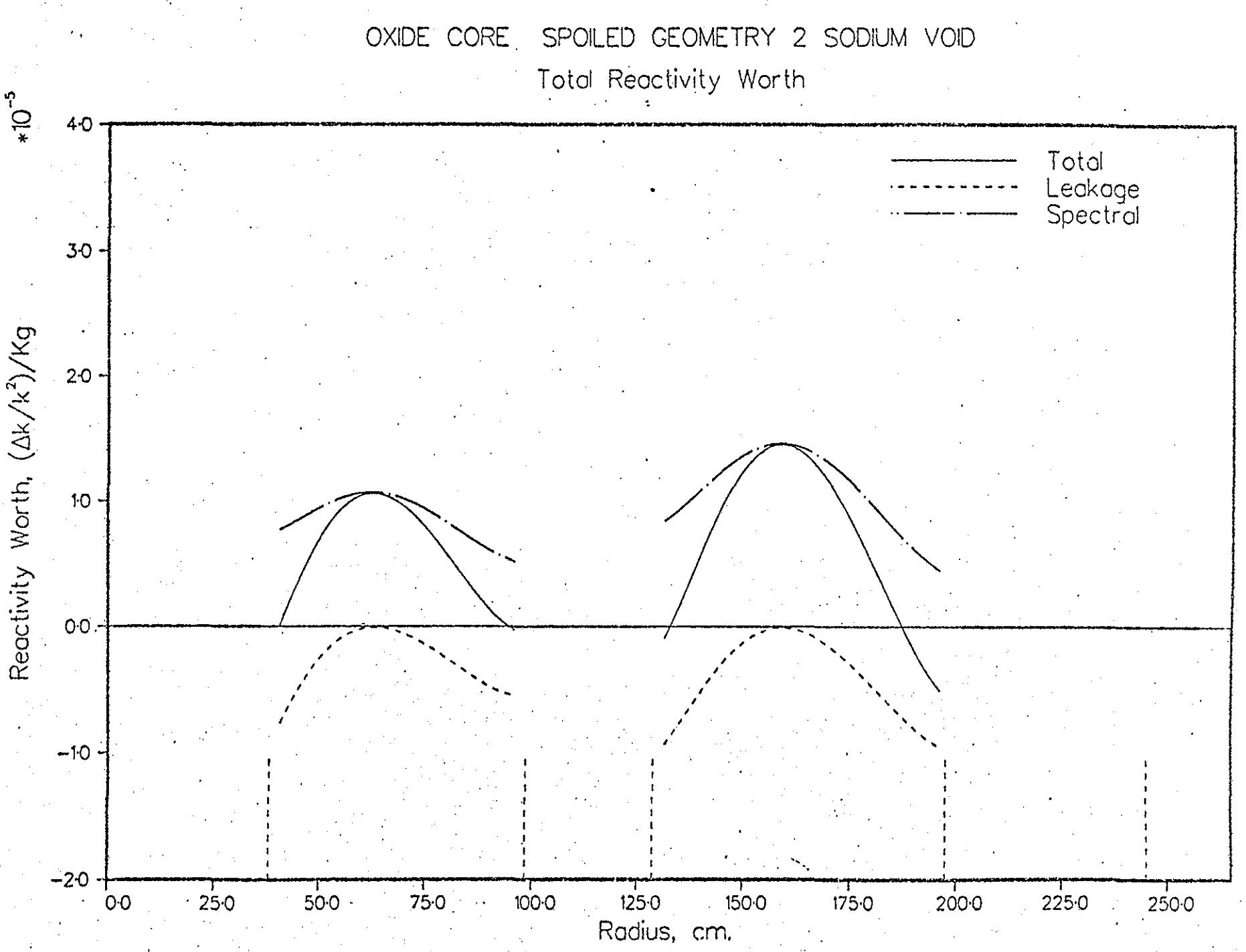

Fig. 7. Core Layout for a 1200 MWe Oxide LMFBR

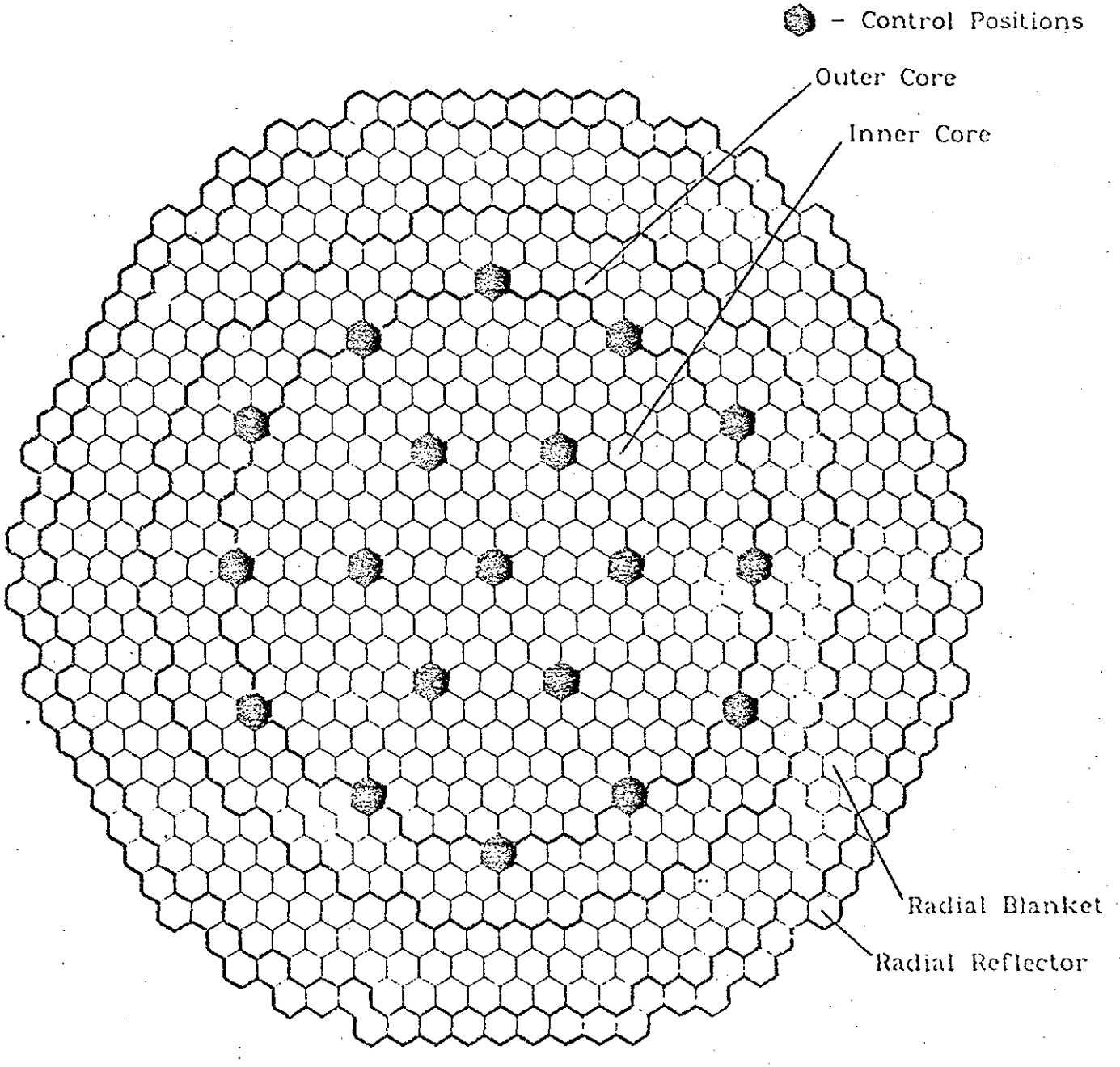

Zone	Number of Assemblies
Core	402
Radial Blanket	252
Radial Reflector	96
Control Positions	19